Transport and magnetic properties of Fe_xVSe_2 (x = 0–0.33)

2008 J. Phys.: Condens. Matter 20 465219

(http://iopscience.iop.org/0953-8984/20/46/465219)

J. Phys.: Condens. Matter **20** (2008) 465219 (6pp) doi:10.1088/0953-8984/20/46/465219

Transport and magnetic properties of Fe_xVSe_2 ($x = 0$–0.33)

C S Yadav and A K Rastogi

School of Physical Sciences, Jawaharlal Nehru University, New Delhi 110067, India

E-mail: shekharjnu@gmail.com and akr0700@mail.jnu.ac.in

Received 28 July 2008, in final form 22 September 2008
Published 27 October 2008
Online at stacks.iop.org/JPhysCM/20/465219

Abstract

We present the results of the effect of Fe intercalation on the structural, transport and magnetic properties of 1T-VSe_2. Intercalation of iron suppresses the charge density wave transition at 110 K in 1T-VSe_2. And for more than 10% Fe concentration a new kind of first-order transition appears below 160 K in our resistivity results. The transition becomes stronger with a broad hysteresis (80–160 K) for 33% Fe intercalation. The anomalies are absent in the thermopower measurements of polycrystalline Fe_xVSe_2 compounds ($x = 0$–0.33). The susceptibility measurements between 2 and 300 K and the magnetization in a high magnetic field up to 14 T at 2 K are reported. The Fe atoms are in the low-spin ($S = 1/2$) state of Fe^{3+} and the compounds show the absence of any magnetic order at low temperatures.

1. Introduction

The layered compounds of group Vb transition metal (V, Nb and Ta) dichalcogenides have been known to show a variety of physical phenomenon like charge density wave (CDW)-related structural distortions, spin density wave (SDW), superconductivity and electronic correlation effects [1–3]. The ambivalent nature of the d-electrons, namely (i) the covalency leads to anisotropic binding with the anions and (ii) the remaining non-bonding electrons show highly correlated metallic behavior that borders the Mott transition, give rise to a rich variety of electronic phase transitions with doping of carriers, external pressure, electric and magnetic fields.

The intercalation of the atoms or substitutional alloying of metal atoms affects the structural and electronic properties of layered compounds differently. The intercalation of relatively small concentrations of atoms often gives a Kondo-like minimum in the resistivity between 10 and 30 K as in 2H-$Fe_{0.05}TaS_2$, 2H-$Fe_{0.05}NbSe_2$ [3], 3R-$Nb_{1.07}S_2$, 3R-Ga_xNbS_2 [4], 1T-$V_{1.1}S_2$ and 3T-$Al_{0.05}VS_2$ [5]. The 5% Fe intercalation in 2H-TaS_2 increases the superconducting transition from 0.8 to 3.3 K, supposedly by suppressing the CDW [3], while with 25% Fe intercalation, it becomes a ferromagnetic metal below $T_c \sim 160$ K and has a large anisotropy and coercive field [6]. On the other hand, with substitutionally alloyed Fe the compound 1T-$Fe_{0.07}Ta_{0.93}S_2$ is diamagnetic at room temperatures. The saturating magnetization behavior at low temperature in this compound is explained as being due to a mixed CDW–SDW state [7]. With the larger amount of Fe substitution in 1T-$Fe_xTa_{1-x}S_2$ ($x < 0.33$) compounds, a dynamic transition from the low-spin to high-spin state has been found on heating to high temperatures [8]. The magnetic property of the Fe-substituted 1T-$V_{1-x}Fe_xSe_2$ with $x \leqslant 1/2$ and its effect on the CDW has been reported by Di Salvo *et al* [9].

In the present study, we have intercalated Fe in 1T-VSe_2 to see the effect of charge transfer on its transport and magnetic properties. The band structure calculations suggest 1T-VSe_2 to be an exchange-enhanced paramagnetic material with a Stoner enhancement factor $S = 4.5$ [10]. As in the case of palladium Fe atoms may also trigger magnetism in 1T-VSe_2. Our studies show the presence of charge transfer effects in the resistivity and thermopower of the Fe_xVSe_2 compound, but even up to 33% concentration of Fe intercalation, the compound remains non-magnetic.

2. Sample preparation

Compounds were prepared by chemical reaction inside a sealed quartz tubes in two stages. VSe_2 and FeSe were first prepared separately by reaction of the pure elements at 700 and 550 °C, respectively. They were then thoroughly mixed in 1:x molar proportions as required for different Fe atom concentrations, pelletized at 5 tons and heat treated at 550 °C for five days. The low temperature of the synthesis and a higher Se content were used to avoid the self-intercalation of V atoms between

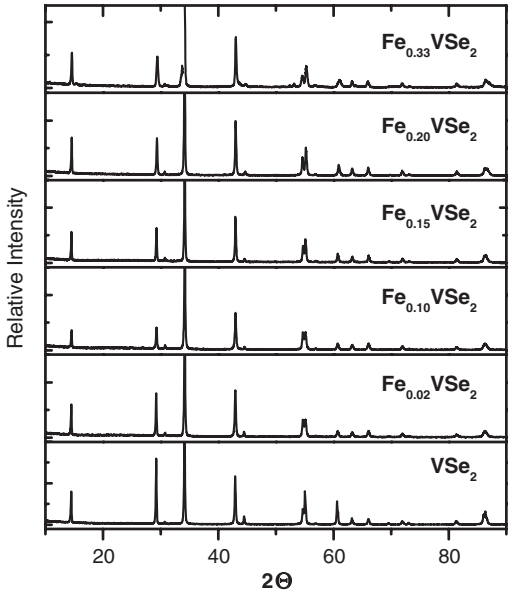

Figure 1. XRD patterns of the LT phases of Fe_xVSe_2 ($x = 0$, 0.02, 0.10, 0.15, 0.20 and 0.33).

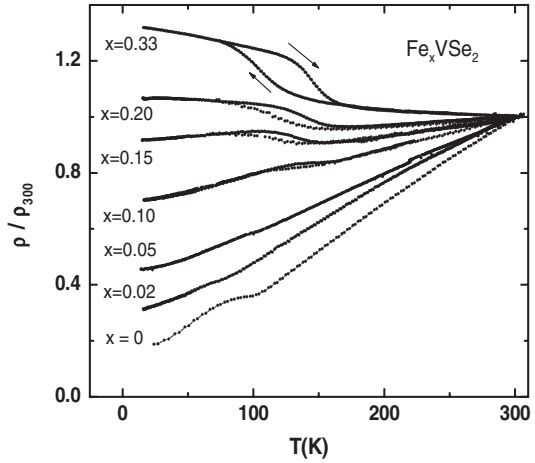

Figure 2. The normalized resistivity plots of polycrystalline Fe_xVSe_2 (LT phases), showing the suppression of the 110 K CDW transition in 1T-VSe_2 for $x \leqslant 0.1$ and a new transition below 160 K for $x = 0.10$–0.33.

the layers of VSe_2. The amount of excess Se used above the Fe_xVSe_2 composition was separated out at the colder end of the tube, as was estimated by weighing the reacted products. A few samples were also sintered at a higher temperature of 700 °C and studied for its possible effects on the transport properties. In a separate preparation, single crystals of VSe_2 and $Fe_{0.33}VSe_2$ ($\sim 3 \times 3 \times 0.02$ mm^3) were obtained by using Se vapor for the transport from 700 to 650 °C in the sealed tubes.

3. X-ray diffraction and structure refinement

The x-ray diffraction pattern of the Fe_xVSe_2 ($x = 0.02, 0.10, 0.15, 0.20, 0.33$) prepared at 550 °C (LT phases) and for $x = 0.20$ and 0.33 prepared at 700 °C (HT phases) are shown in figure 1. Up to 20% intercalation of Fe, no visible changes in the peak patterns are observed, except for the expected changes in relative intensity. The slight broadening of lines and the additional weak peaks in the 33% Fe intercalated compound may be related to structural distortion due to the short range ordering of the Fe atoms. The precise lattice parameters of these compounds were obtained using Crysfire software [11, 12] and are listed in table 1.

We see from table 1 that, for small Fe intercalation, the lattice parameters remain unchanged from that of 1T-VSe_2 ($c = 6.104$ Å and $a = 3.356$ Å). And for more than 10% Fe atoms, the structure starts deviating from the hexagonal to orthorhombic and monoclinic, the decrease in c and increase in a parameters leading to the consistent reduction in the c/a value with increasing Fe intercalation.

For the LT 33% Fe intercalated compound, the ordering of Fe leads to the superstructure formation with lattice parameters $a = 3.527$ Å, $b = 5.819$ Å ($\sqrt{3} \times 3.360$) and $c = 12.14$ Å (2×6.07). On the other hand, high temperature synthesis stabilizes the hexagonal structure both for $x = 0.20$ and 0.33.

Table 1. Lattice parameters of Fe_xVSe_2.

Fe_xVSe_2 x	a (Å)	b (Å)	c (Å)	V (Å^3)	Comment
0.00	3.356	3.356	6.104	59.57	Hexagonal
0.02	3.356	3.356	6.100	59.54	Hexagonal
0.10	3.351	5.814	6.097	118.77	Orthorhombic
		$\sqrt{3} \times 3.567$		$Z = 2$	
0.15	3.357	5.808	6.097	118.86	Orthorhombic
		$\sqrt{3} \times 3.353$		$Z = 2$	
0.20	3.359	5.764	6.081	117.7	Monoclinic
(LT)		$\sqrt{3} \times 3.328$		$\gamma = 91.5$	
0.20	3.351	3.351	6.090	59.234	Hexagonal
(HT)					
0.33	3. 353	5.819	2×6.074	249.6	Monoclinic
(LT)		$\sqrt{3} \times 3.360$		$\gamma = 91.6$	
0.33	3.365	3.365	6.056	59.36	Hexagonal
(HT)					

The absence of distortion here is most likely related to the disorder caused by the interlayer mixing of some V and Fe atoms in our HT phases.

4. Transport properties

4.1. Electrical resistivity

The electrical resistivity of the polycrystalline pellets of Fe_xVSe_2 was measured from 2 to 300 K. The results of all of them are plotted in figure 2 after normalizing the respective resistances at room temperature. It is seen that the metal-like temperature dependence changes to insulator-like with increasing Fe concentration. 1T-VSe_2 shows a distinct anomaly in the temperature coefficient of the resistance of the polycrystalline pellet at the onset of CDW at 110 K. The CDW anomaly is reduced and completely suppressed for the $x \geqslant 0.1$ concentration of intercalated iron. We can compare this effect of intercalation with the much more rapid suppression of CDW in the case of substitutional alloying of Fe in 1T-$V_{1-x}Fe_xSe_2$, where the magnetic susceptibility results showed

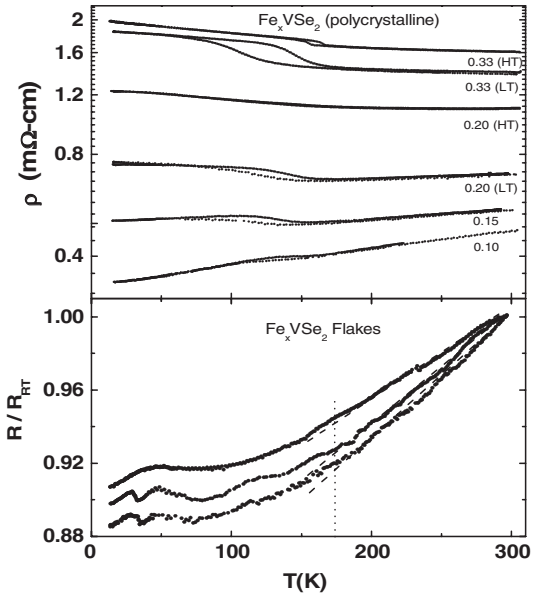

Figure 3. Electrical resistivity of polycrystalline Fe_xVSe_2 ($x = 0$, 0.10, 0.15, 0.20, 0.33) (upper panel) and Fe_xVSe_2 flakes (lower panel), showing the anomaly around 160 K transition.

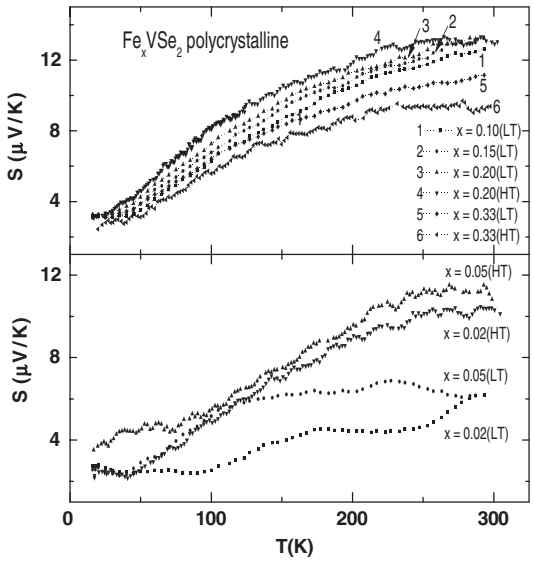

Figure 4. Temperature dependence of the thermopower of polycrystalline Fe_xVSe_2; $x = 0.02$, 0.05 (lower panel) and $x = 0.10$, 0.15, 0.20, 0.33. HT and LT written in parentheses denote the high temperature and low temperature phases of the compounds, respectively.

its elimination for $x > 0.035$ [9]. The most important observation is that, for more than 10% Fe concentration, a new kind of first-order transition appears at 160 K and the resistivity showed a hysteresis on cooling and warming. This hysteresis becomes broader for the $x = 0.33$ compound (LT phase) in which our x-ray diffraction analysis gave a marked distortion of the crystal structure.

In figure 3, we have plotted the resistivity of the Fe_xVSe_2 polycrystalline, including the HT phases between 15 and 300 K in the upper panel and some Fe_xVSe_2 crystal flakes ($x =$ unknown) in the lower panel. The crystal flakes were obtained by the transportation of $Fe_{0.33}VSe_2$ using Se vapor from 700 to 650 °C and may have variable Fe concentrations.

In the upper panel we can see that the jump in the resistivity and the transitional hysteresis at 160 K is considerably reduced in the hexagonal HT phases. In both of these the interlayer mixing of V and Fe gave the distortion of the parent hexagonal structure.

Unlike the case of polycrystalline pellets, where resistivity rises on lowering the temperature, the flakes show metal-like temperature dependence. We believe that this difference is due to the anisotropic nature of the conductivity of our intercalated compounds: the *ab*-plane conductivity of flakes is large and metallic, while the intercalation leads to an increase in the degree of localization perpendicular to the *ab* planes and an insulating-like temperature dependence on cooling as found in the polycrystalline pellets.

Although in the flakes of Fe_xVSe_2 a metal-like dependence is found, a vestige of the 160 K anomaly can also be noticed. The drop in resistance on cooling is considerably reduced below 160 K, as seen in the figure below the dotted lines, and a clear resistance minimum is found at 80–100 K. On further cooling, the resistivity of the crystal flakes shows a sharp downward trend after 50 K. At present, we have no explanation for this type of behavior in our flakes.

4.2. Thermoelectric power

The temperature dependence of the thermoelectric power (TEP) of the polycrystalline Fe_xVSe_2 compounds is shown in figure 4. In a separate panel, we have shown the TEP for $x = 0.02$ and 0.05 compounds, which were prepared at two different temperatures, namely 550 °C (LT phase) and 700 °C (HT phase). For all the compositions, thermopower is positive and varies from 2 μV K^{-1} at 15 K to a nearly saturated value of 8–13 μV K^{-1}, at room temperature.

In the lower panel of the figure, TEP of the HT phases has a higher value and, except for a sharp change in slope at the temperatures around 70 K, the TEP dependence for $x = 0.02$ and 0.05 is similar to their higher concentration counterpart.

For the higher concentration phases shown in the upper panel of figure 4, TEP increases with concentration, irrespective of their preparation conditions and thus shows the effect of charge transfer from intercalated Fe to the host V atom. The exception being $Fe_{0.33}VSe_2$, for which TEP lies at the lowest values. The reduction may be related to the ordering of Fe atoms for $x = 1/3$. This ordering can be instrumental in distorting the topology of the Fermi surface, causing a change in the thermopower.

The Seebeck coefficient (S) or the TEP of metallic electrons, suffering elastic scattering at a temperature T, is given by the Mott expression [13]:

$$S = \frac{\pi^2}{3}\frac{k_B^2}{e}T\left(\frac{\partial \ln \sigma}{\partial \varepsilon}\right)_\eta \qquad (1)$$

where k_B = Boltzmann constant, e = charge of electron, σ = electrical conductivity of electrons of energy ε and η is the chemical potential of electrons.

In figure 5, we have plotted S/T as a function of temperature to see if anomalies in TEP due to the 160 K

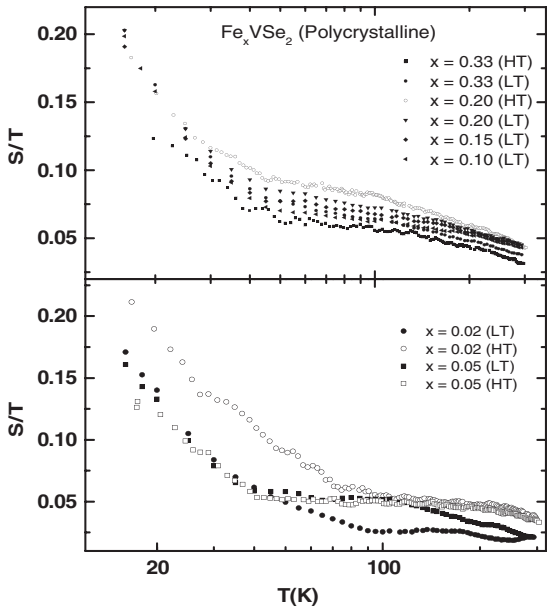

Figure 5. Temperature dependence of the Seebeck coefficient of polycrystalline Fe_xVSe_2 plotted as S/T versus Log T. $x = 0.02$, 0.05 (lower panel) and $x = 0.10$, 0.15, 0.20, 0.33 (upper panel).

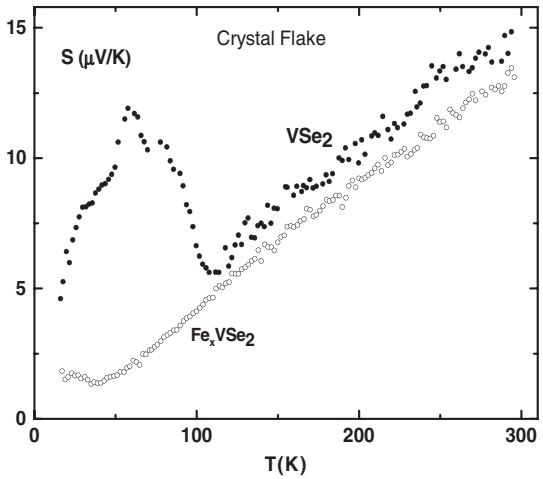

Figure 6. The Seebeck coefficient of the 1T-VSe_2 and Fe_xVSe_2 crystal flakes.

transition are present. For any Fermi-surface-related instability the derivative of conductivity with respect to energy is expected to change, thus affecting S, as is expected from the above relation (1). We can see some effects of the 160 K transition as, in the upper panel, for higher Fe concentrations ($x = 0.10$–0.33), S/T rises linearly on cooling and changes its slope in the region 80–170 K. Whereas for $x = 0.02$–0.05 compounds (LT phases) without 160 K anomalies in resistivity in the lower panel, S/T remain nearly constant till 40 K, as expected for the thermopower of metallic conduction.

It is interesting to note in figure 6 that the thermopower of crystal flakes shows a qualitatively different behavior on temperature. A sharp transition is seen at the CDW transition of 1T-VSe_2. But the TEP of Fe_xVSe_2 crystal flakes neither show the 110 K CDW transition, as in the VSe_2 flake, nor does it show any signature of the 160 K transition. Instead, it shows a pure metallic behavior down to 30 K.

5. Magnetic properties

In figure 7, we have shown the temperature dependence of the susceptibility of Fe_xVSe_2 ($x = 0.02$, 0.05, 0.20 and 0.33), measured at 1 T magnetic field. The data are fitted to the Curie–Weiss formula:

$$\chi = \chi_0 + \frac{C}{T + \theta}. \tag{2}$$

The values of different parameters—χ_0 (the temperature-independent contributions to susceptibility from V bands), C (the Curie constant of Fe moments) and θ (antiferromagnetic Néel temperature)—obtained from the fitting are listed in table 2. We find a definite increase in the value of χ_0 on increasing Fe concentration. The effective paramagnetic moments calculated from the Curie constant are in the range of 1.69–1.05 μ_B per Fe atom. This value is closer to the value

Table 2. The magnetic parameters of Fe_xVSe_2.

Compound	χ_0 10^{-4} (emu mol^{-1} K^{-1})	$C_{\text{per Fe}}$ (emu mol^{-1} K^{-1})	$\mu_{\text{eff/Fe}}$ (μ_B)	θ_N (K)
$Fe_{0.02}VSe_2$	3.4	0.36	1.69	5.7
$Fe_{0.05}VSe_2$	3.4	0.30	1.55	5.9
$Fe_{0.20}VSe_2$	4.8	0.14	1.05	6.8
$Fe_{0.33}VSe_2$	4.7	0.23	1.35	8.0

of the effective moment of 1.73 μ_B for one unpaired electron ($S = 1/2$) per Fe atom and which correspond to the low-spin state of the Fe^{3+} ($3d^5$) oxidation state. Our results for the low-spin state of the intercalated Fe atoms in VSe_2 are also consistent with the previous study of substitutional alloying of V atoms by Fe in 1T-$V_{1-x}Fe_xSe_2$ by DiSalvo *et al* [9, 14]. Here the substituted Fe atoms had no moments and the small effective moments of 0.6 μ_B found for $x = 1/2$ and 1/3 were attributed to the unavoidable interstitial Fe or V atoms present in these compounds, which have $S = 1/2$ and 1 moments, respectively.

We also observe a small jump-like anomaly in the susceptibility of $Fe_{0.33}VSe_2$ at the 160 K transition. This seems to be related to the anomalies observed in the resistivity of this compound at the same temperatures. The magnetic behavior of $Fe_{0.33}VSe_2$ has been discussed and analyzed in detail in our separate study [14].

We have measured the field dependence of the magnetization of Fe_xVSe_2, $x = 0.02$, 0.05, 0.20 and 0.33, samples up to 14 T field at 2 K temperature. Our results are shown in figure 8. The magnetization of these compounds shows a continuous downward curvature even at the highest fields of 14 T. This behavior does not permit the separation of a linear term (due to Pauli paramagnetism χ_0 of the V bands) and a saturated moment of localized Fe or V electrons. We believe that, the same as in pure VSe_2, the V-band electrons show considerable exchange enhancement of χ_0 after the charge transfer from Fe atoms. Thus a nonlinear $M(H)$ dependence is expected from the Stoner model of band magnetism. The localized d-electrons of Fe atoms being in the low-spin state cannot lead

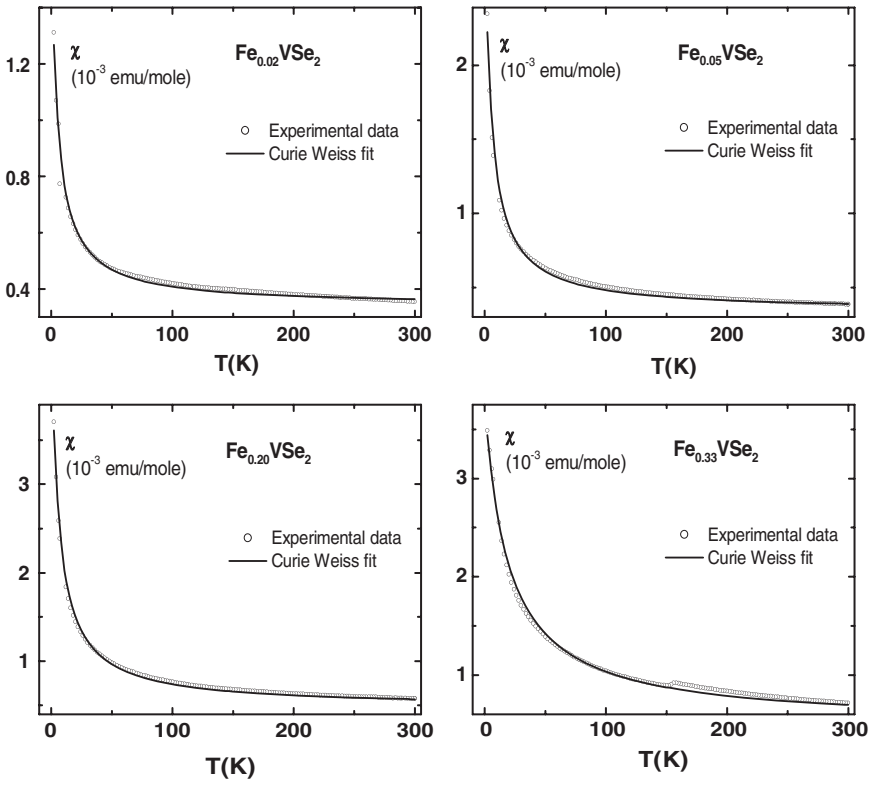

Figure 7. The temperature dependence of the susceptibility of the Fe_xVSe_2, measured at 1 T magnetic field. Curie–Weiss fit of the data is also shown in the figure.

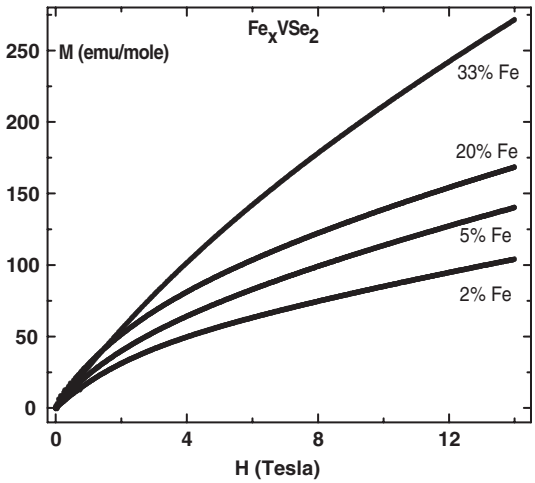

Figure 8. Magnetization of Fe_xVSe_2 at 2 K showing non-saturating behavior in all of them up to 14 T field.

to the fulfillment of the Stoner criterion of band polarization and magnetic order in these compounds.

6. Conclusion

We observed the effect of Fe intercalation on the properties of the 1T-VSe_2 compound. The intercalation of Fe suppresses the 110 K CDW transition and a new first-order transition appears at 160 K, which gets stronger for higher Fe intercalation, especially for the phases prepared at low temperatures. The contrasting behavior of the resistivity of Fe_xVSe_2 crystal flakes (metallic-like in the *ab* planes) to that of the polycrystalline samples (insulating-like along the *c* axis) is due to considerable anisotropy of electronic transport in these compounds. In the polycrystalline samples the localization of the *c*-axis resistivity increases on increased intercalation and also on cooling to low temperatures. Thus in these intercalated compounds, the anisotropy of transport increases on cooling.

The thermopower of the compounds does not show any visible anomaly around the transition, except for the systematic change in the magnitude of the thermopower on Fe intercalation. The Seebeck coefficient (see relation (1)) is a function of $\sigma(\varepsilon)$ and is very sensitive to the inelastic scattering near the Fermi energies. The absence of significant anomalies in the thermopower in our compounds at the 160 K transition indicate that this transition does not cause significant changes in the Fermi surface. Thus we rule out CDW-related instability at 160 K in Fe_xVSe_2. The anomalies in the resistance, on the other hand, show the effects on the mobility of the electrons, which are increasingly localized along the *c* axis of the crystallites in our polycrystalline samples. We find that this localization is quite sensitive to the structural distortions and preparation conditions. We also observe that the jump and the hysteresis of the transition are eliminated in our undistorted hexagonal phases obtained by high temperatures synthesis.

Fe_xVSe_2 does not show any saturation of magnetization even in 14 T magnetic fields and remains a weak paramagnetic. The picture of itinerant band magnetism seems more

appropriate for this system. We started this work with the presumption that the presence of Fe atoms may trigger the magnetism in the narrow d-band of the 1T-VSe_2 compound. Our magnetic study indicates that the intercalated Fe is in the low-spin state with $S = 1/2$ of Fe^{3+}. With this low moment the possibility of induced ferromagnetism in the VSe_2 is negated, at least for Fe concentrations up to 33%. The calculation of the crystal field effect on the Fe moments can give a detailed picture of the magnetism and moment variation in these compounds.

Acknowledgment

CSY acknowledges the Council of Scientific and Industrial Research (CSIR) India for the Senior Research fellowship.

References

[1] Friend R H, Beal A R and Yoffe A D 1977 *Phil. Mag.* **35-5** 1269
[2] Parkin S S P and Friend R H 1980 *Phil. Mag.* **41-1** 65
Parkin S S P and Friend R H 1980 Transport properties *Phil. Mag.* **41-1** 95
Parkin S S P and Friend R H 1980 Optical properties *Phil. Mag.* **42-5** 627
[3] Whitney D A, Fleming R M and Coleman R V 1977 *Phys. Rev.* B **15** 3405
[4] Niazi A and Rastogi A K 2001 *J. Phys.: Condens. Matter* **13** 6787
[5] Poddar P and Rastogi A K 2002 *J. Phys.: Condens. Matter* **14** 2689
[6] Morosan E, Zandbergen H W, Li L, Lee M, Checkelsky J G, Heinrich M, Siegrist T, Ong N P and Cava R J 2007 *Phys. Rev.* B **75** 104401
[7] Dai S, Yu C, Li D, Shen Z, Fang S and Jin J 1995 *Phys. Rev.* B **52** 1578
[8] Eibsuitz M and Disalvo F J 1976 *Phys. Rev. Lett.* **36** 104
[9] DiSalvo F J and Waszczak J V 1976 *J. Physique* **37** C4 157
[10] Myron H W 1980 *Physica* B **99** 243
[11] Shirley R 2002 *The Crysfire 2002 System for Automatic Powder Indexing: User's Manual* (Guildford: The Lattice Press)
[12] Tauplin D 1979 *J. Appl. Crystallogr.* **6** 380
[13] Mott N F and Jones H 1936 *The Theory of the Properties of Metals and Alloys* (Oxford: Clarendon)
[14] Yadav C S and Rastogi A K 2008 *J. Phys.: Condens. Matter* **20** 415212